



Development of an anatomical breast phantom from polyvinyl chloride plastisol with lesions of various shape, elasticity and echogenicity for teaching ultrasound examination

Denis Leonov^{1,2} · Daria Venidiktova³ · José Francisco Silva Costa-Júnior⁴ · Anastasia Nasibullina^{1,2} · Olga Tarasova⁵ · Kristina Pashinceva⁶ · Natalia Vetsheva⁷ · Julia Bulgakova^{1,2} · Nicholas Kulberg⁸ · Alexey Borsukov³ · Manob Jyoti Saikia⁹

Received: 5 January 2023 / Accepted: 4 April 2023
© CARS 2023

Abstract

Purpose The WHO reported an increasing trend in the number of new cases of breast cancer, making it the most prevalent cancer in the world. This fact necessitates the availability of highly qualified ultrasonographers, which can be achieved by the widespread implementation of training phantoms. The goal of the present work is to develop and test an inexpensive, accessible, and reproducible technology for creating an anatomical breast phantom for practicing ultrasound diagnostic skills in grayscale and elastography imaging, as well as ultrasound-guided biopsy sampling.

Methods We used FDM 3D printer and PLA plastic for printing an anatomical breast mold. We made a phantom using a mixture of polyvinyl chloride plastisol, graphite powder, and metallic glitter to simulate soft tissues and lesions. Various degrees of elasticity were imparted using plastisols of stiffness ranging from 3 to 17 on the Shore scale. The lesions were shaped by hand. The materials and methods used are easily accessible and reproducible.

Results Using the proposed technology, we have developed and tested a basic, differential, and elastographic versions of the breast phantom. The three versions of the phantom are anatomical and intended for use in medical education: the basic version is for practicing primary hand–eye coordination skills; the differential one is for practicing the differential diagnosis skills; the elastographic version helps developing the skills needed for assessing the stiffness of tissues.

Conclusion The proposed technology allows the creation of breast phantoms for practicing hand–eye coordination and develop the critical skills for navigation and assessment of the shape, margins, and size of the lesion, as well as performing an ultrasound-guided biopsy. It is cost-effective, reproducible, and easily implementable, and could be instrumental in generating ultrasonographers with crucial skills for accurate diagnosis of breast cancer, especially in low-resource settings.

Keywords Training phantom · Breast ultrasonography · Ultrasound · Tissue-mimicking materials · PVC plastisol · Mammary gland

Introduction

According to the WHO, there were 2.3 million women diagnosed with breast cancer and 685,000 deaths globally in 2020. As of the end of 2020, there were 7.8 million women alive who were diagnosed with breast cancer in the past 5 years, making it the world's most prevalent cancer in women. Ultrasound examination plays an important role in the diagnosis of cancer, since this method allows experienced clinicians to differentiate malignant from benign lesions with great certainty based on the assessment of size,

shape, elasticity, and echogenicity [1]. In addition, compared to mammography equipment, ultrasound equipment is more affordable and portable. Consequently, routine breast cancer screening with ultrasound devices is cheaper and more feasible in low-resource settings. As opposed to mammography using X-rays, ultrasound uses no ionizing radiation and does not cause pain or discomfort by compressing the breasts.

However, the diagnostic accuracy depends on the qualification and experience of ultrasonographers [2]. Therefore, it is important that the scientific community and healthcare institutions make efforts to develop and use tools for training highly qualified specialists by not only theoretical teaching but also practicing at the clinical sites ideally involving real

Extended author information available on the last page of the article

patients. However, intensive training on real patients is neither feasible nor desirable due to ethical constraints. In recent years, one of the tools that has gained prominence in the medical community is the ultrasonic phantom, which is made of tissue-mimicking materials that present morphological and acoustic properties close to human tissues [3, 4]. Undoubtedly, ultrasonic phantoms are essential in medical education and training because, in many situations, they make possible the replacement of training on real patients, cadavers, and animals. Medicine students can learn to identify specific types of lesions in phantoms using ultrasonic imaging, and practice repeatedly to improve their skills without any constraint. The characteristics of the ultrasonic images obtained from the phantom depend on the materials used to build and the manufacturing process. The following materials are most often used for simulating acoustic properties of breast tissues: chicken breast [5] and biopolymers [6, 7], characterized by the low cost and ease of manufacturing, but low durability; polyvinyl alcohol cryogel [8], which allows controlling acoustic parameters using freezing cycles; polyacrylamide [9], which emits toxic fumes during the manufacturing process; and polyvinyl chloride plastisol [10–15], and silicone [16], characterized by resistance to fungi and bacteria, durability and ease of use.

This article presents the design of three training breast phantoms using polyvinyl chloride plastisol. We call them basic, differential and elastographic breast phantoms. The basic phantom contains lesions of such shapes that are recognizable even to novice students. This phantom was designed for those students who wish to train their hand–eye coordination with almost no supervision from an instructor. The differential phantom contains lesions that are similar in shape, echogenicity, and elasticity to the common breast lesions such as lipoma, fibroadenoma, malignant tumor, and cyst. This phantom helps practice skills of differential diagnostics. The elastographic phantom contains spherical lesions with different levels of hardness, which can be used for practicing elastography skills.

The main contribution of this work in relation to other publications involving polyvinyl chloride plastisol as a tissue-mimicking material [10–15] is that it presents a method for designing phantoms and models of lesions, which are not only closely reproduce shape but also echogenicity and elasticity of abnormal changes in the breast tissue. Since the phantoms are permeable to the needle and contain lesions of various shapes and sizes, echogenicity, and elasticity, they can be used for practicing ultrasound examination skills and needle-insertion procedures under ultrasound guidance.

Materials and methods

3D printer

A 3D printer (Designer X Pro, Picaso 3D, Moscow, Russia) operating on FDM technology was used to make the casting molds for the breast phantoms. The printer is equipped with a heated table and enclosed build chamber with the printable area of $200 \times 200 \times 210$ mm and optimal layer thickness of 50 microns for professional modeling.

Tissue-mimicking materials

Plastisols (Redbug, Dmitrov, Russia) were used as the main material for manufacturing phantoms. Plastisols were differed in stiffness (Young's modulus), expressed as a value on the Shore stiffness scale, as well as in the type of admixture and its concentration. Unlike biopolymers, in particular mixtures of gelatin and agar, plastisols are durable, easy to store and use. Furthermore, it is a nontoxic, nonpolluting, and low-cost material [1].

The structure of pure plastisol contributes a small amount of scattering, so to make the speckle pattern image of this type of material closer to that obtained in the highly scattering human tissue, it is necessary to add scatterers to the plastisol. There are studies in the literature that used scatterers such as titanium dioxide (TiO_2) and glass microspheres [17], aluminium oxide (Al_2O_3) and graphite powders [13]. The ultrasonic images obtained in the breast phantoms presented in those works were close to the images obtained in human breasts, so the scatterers employed are quite promising. However, there is no study that compared speckle patterns produced by different scatters and demonstrates the most appropriate admixtures for ultrasonic phantoms.

In this work, the comparison of speckle patterns was made (Fig. 1). We used graphite powder and metallic glitter as scatterers. By changing their concentration in relation to plastisol, we managed to create a grayscale “palette” in which we reproduced hypoechoic and hyperechoic tissues as well as tissues of intermediate echogenicity (Fig. 1). It was obtained using an ultrasound equipment (Sonoace 8000 EX Prime; Medison Co., Seoul, South Korea) with the L5-9EC probe operating at the center frequency of 7.5 MHz. In this palette, we used the gradation of echogenicity as described in the caption for Fig. 1. Graphite powder with a particle size of 40–80 μm (SpheroLit company, Smolensk, Russia) consisted of 79% carbon, 23% ash, 0.34% Sulphur and 1% moisture. Heat-resistant metallic glitter particles (Redbug, Dmitrov, Russia) had a size of 200 μm . The influence of the admixture on the acoustic properties (attenuation coefficient and ultrasonic speed) was evaluated.

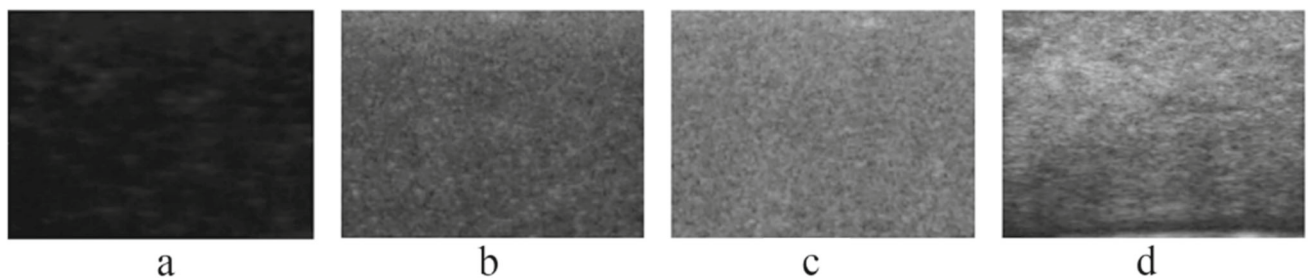


Fig. 1 Ultrasound images of the samples of polyvinyl chloride plastisol ranked in order of increasing echogenicity creating a grayscale palette: **a** level 1—no admixture; **b** level 2—with the addition of 0.5% graphite

powder; **c** level 3—with the addition of 1% graphite powder; **d** level 4—with the addition of 1% graphite powder and 0.5% metallic glitter

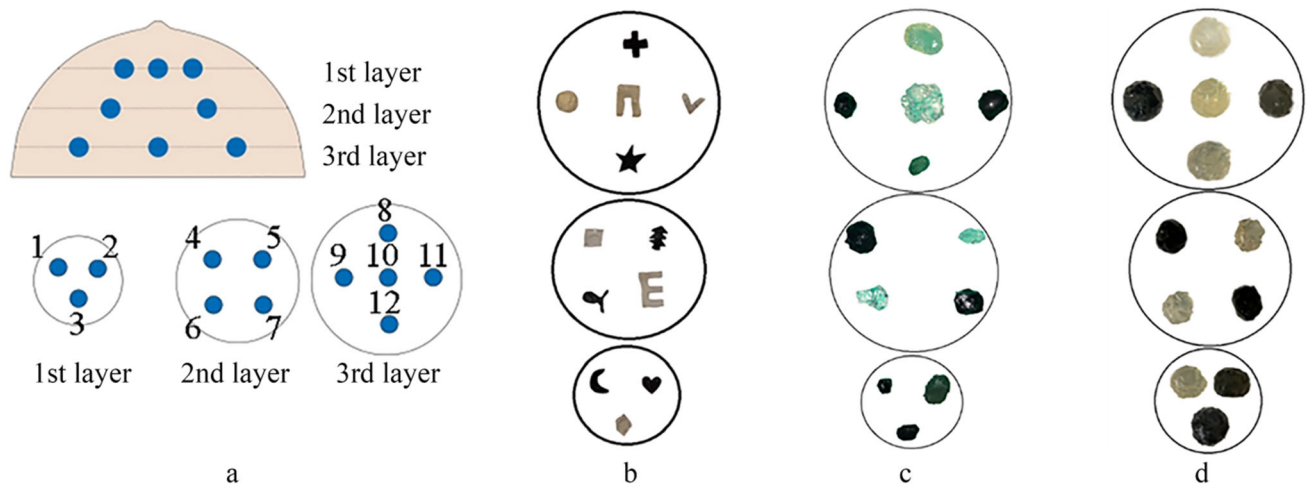


Fig. 2 Lesions in the breast phantom: **a** layout; **b** lesions of the basic version; **c** lesions of the differential version; **d** lesions of the elastographic version

Breast phantoms

Three breast phantoms were prepared in this study: basic, differential, and elastographic. Each phantom was 165 cm in length and contained 12 lesions, arranged according to the scheme shown in Fig. 2. We shaped the lesions by hand using nail scissors. They were cut out from bars 70 × 30 × 30 mm in size, which were made from polyvinyl chloride plastisol with graphite powder and metallic glitter as admixtures. The first version of the phantom, the basic one, had a background with level 3 echogenicity and hardness of 9 Shore scale units. It contained lesions that were not similar to real lesions in shape but had recognizable outlines. The purpose of this phantom is to train basic navigation skills, assessing the shape, contour, and size of the lesion, as well as carrying out an ultrasound-guided biopsy. In the second version of the phantom, differential, a background had the level 3 echogenicity and hardness of 11 units. It contained imitations of lesions having the shape, echogenicity, and elasticity of the real ones, namely a simple cyst (5, 8), lipoma (1, 7), fibroadenoma (2, 12), fibrolipoma (4, 9), and malignant

tumor (3, 6, 10, 11). Thus, the differential version contains anthropomorphic masses and is intended to improve the differential diagnosis skill of breast tumors. The third version of the phantom, elastographic, had a background with level 4 echogenicity and hardness of 6 units. It contained masses of various stiffnesses and designed for elastography training. Half of the masses in the elastographic version was hypochoic, and the other half was isochoic, so that they could be detected only in the elastography mode.

The stiffness of lesions and breast tissue in phantoms was modeled using different polyvinyl chloride plastisols. They differ in their concentration of plasticizer. The greater the concentration the stiffer is the tissue-mimicking material [15]. The manufacturer provided us with data on the plastisol stiffness in units on the Shore stiffness scale, which along with other characteristics of the modeled inclusions is given in Fig. 3. Lesions 3 and 11 in the differential phantom model tumors with irregular borders. Their outer layer is 3 times harder and slightly dimmer than the inner layer.

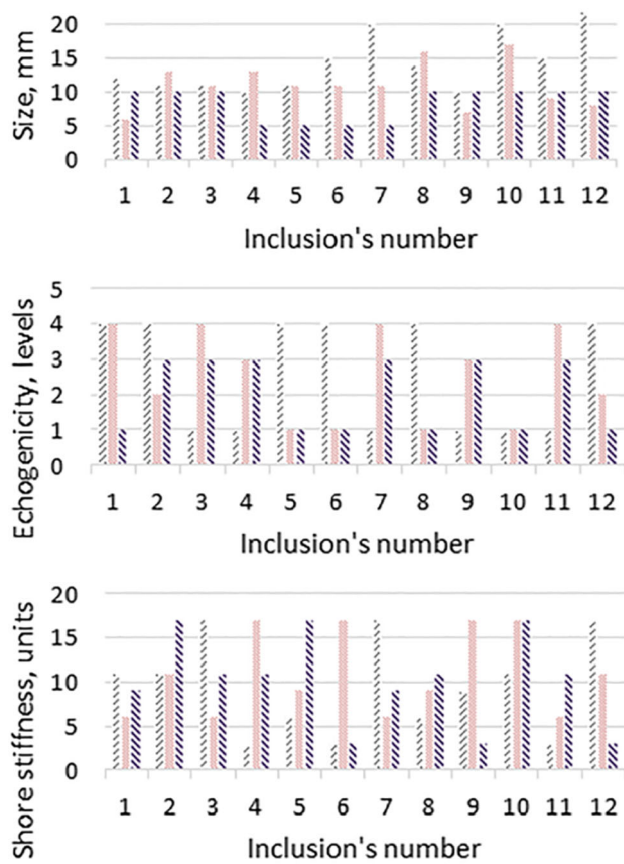


Fig. 3 Characteristics of inclusions in the basic (▨), differential (■) and elastographic (▨) versions of the breast phantom

Phantom mold and manufacturing process

3D modeling software program Meshmixer (Autodesk Inc., San Rafael, CA, USA) was used for creating a casting mold for the phantom. Based on the analysis of computer tomograms of breasts regularly performed for numerous patients, a reconstruction of the typical breast contour was performed in this program. For the stability of the structure and the convenience of manufacturing the phantom, a rectangular case with dimensions of $180 \times 140 \times 70$ mm was built around the model (Fig. 4a and b). The obtained mold model was saved in STL file format and was made available to those who wish to replicate our experiments [18]. We have chosen PLA plastic for printing a casting mold for several reasons, namely this material does not chemically interact with plastisol, is suitable for manufacturing sealed structures, and withstands an operating temperature of at least 160°C .

A plastisol is a colloidal dispersion of small polymer particles in a liquid plasticizer. When heated to around $160\text{--}180^\circ\text{C}$ ($320\text{--}356^\circ\text{F}$), the plastic particles absorb the plasticizer, causing them to swell and fuse together forming a viscous gel [19]. Once the solution is cooled to below 60°C

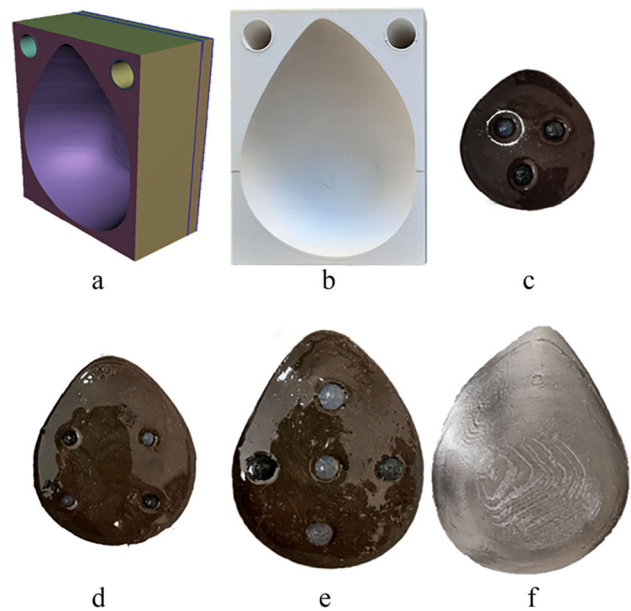


Fig. 4 Stages of phantom manufacturing: **a** creating a virtual model; **b** 3D-printing the mold; **c** filling the 1st layer and adding 3 lesions; **d** filling the 2nd layer and adding 4 lesions; **e** filling the 3rd layer and adding 5 lesions; **f** phantom after removal from the mold

(140°F) it becomes a flexible, permanently plasticized solid product. This process is called 'curing'.

For heating, it is necessary to use a thick-walled ceramic container, in which a plastisol can cool down more slowly. A microwave oven is most convenient for heating as it heats the substance evenly. When plastisol is stored in the liquid form for a long time, a precipitate occurs at the bottom of the bottle. In order to dissolve it, it is necessary to shake the contents for 2–3 min before use. Then pour a liquid plastisol into the container and put it in the oven. It is necessary to use the moderate power in the oven and to stop the heating for 15 s every 30 s in order to mix the substance thoroughly. During the heating process, the plastisol gets thicker first, and then becomes very fluid again. When the temperature reaches 150°C , it is necessary to wait at least for a minute in order to let the air bubbles escape from the solution. Overheating of the plastisol should be avoided, as this leads to burning and damaging the material. The temperature was measured using a digital thermometer Fantast (IKEA, Sweden).

When the temperature reached 160°C , the resulting mixture was poured into the prepared breast mold, shown in Fig. 4b. The filling process was performed in layers. The thickness of each layer was 20 mm. We placed the lesions in 3 layers according to the scheme shown in Fig. 1. The filling process is illustrated with photos 3c–e. After filling a layer, but before placing the lesions, we waited for about 30 s for the formation of a film that prevents the lesions from drowning. After filling the last layer, we left the phantom at the room temperature until it cooled down completely. After that, we

took it out of the mold. Upon completion of the described process, the phantom is ready for use and looks as shown in Fig. 4e.

Characterization of acoustic properties

In order to select suitable materials, admixtures and their concentrations, an experiment was carried out to estimate the speed and attenuation coefficient of ultrasonic waves. We employed a relative measurement method previously used in [20] to study the transmission of longitudinal ultrasonic waves through solid media. The experimental setup consists of an ultrasound source and a hydrophone coupled with gel to the sides of a sample in the form of a rectangular parallelepiped. Each sample was made from polyvinyl chloride plastisol having different concentrations of admixtures by the size of $70 \times 30 \times 30$ mm. The ultrasonic signals were generated and collected by A1550 Intro Visor Ultrasonic flaw detector (Acoustic Control Systems—ACS Group, Saarbrücken, SL, Germany). Two S3568 sensors with a center frequency of 2.5 MHz having piezo elements with a diameter of 10 mm were coupled to the flaw detector and served as the ultrasound source and the hydrophone. The source emitted a burst at a carrier frequency in the range from 1 to 5 MHz with 25 V and a pulse repetition frequency of 10 Hz. The source and the hydrophone were located coaxially on both sides of the sample. The ultrasonic signal emitted by the source passed through the sample and was collected by the hydrophone with the same central frequency and sampled with a sampling frequency of 60 MHz. The measurements were carried out for the rectangular cuboid sample with transducers coupled to its sides so that there was a 30 mm distance between the surfaces of the transducers. Then the sensors were coupled to other sides so that a 70 mm distance was between the sensors' apertures and the measurements were repeated. The unknown sound velocity in each sample was deduced from the temporal shift between the pulse transmission times for the 30 mm and 70 mm distances between the apertures using the equation:

$$c = \frac{l_1 - l_2}{t_1 - t_2}, \quad (1)$$

where l_1 and l_2 are the distances between the coaxially placed ultrasound source and hydrophone equal to 30 and 70 mm, respectively, *i.e.*, the length and width of the rectangular parallelepiped samples; t_1 and t_2 are time intervals between emission and arrival of ultrasound pulses traveling through the samples for the 30 and 70 mm distance, respectively. The probing pulse had an envelope with a Gaussian shape and a length of 5 cycles. Time was measured at the peak value of the envelope. The attenuation coefficient α was calculated from the difference in the amplitude of the signals received

for two distances between sensors' apertures:

$$\alpha = \frac{20 \log_{10} \left(\frac{A_1}{A_2} \right)}{l_1 - l_2}, \quad (2)$$

where A_1 and A_2 are the peak values of the envelopes of the received signals for the two measurements, carried out for the distances l_1 and l_2 , 3 and 7 cm, thus the α is measured in dB/cm. The attenuation coefficient was estimated using signals with a 1 MHz carrier frequency. The experiments were conducted at a temperature of 24.0 ± 0.1 °C, which was monitored using a digital thermometer TPM-10 (ESPADA, Moscow, Russia). Prior to applying this technique, the Eqs. (1) and (2) for estimating the speed of sound and attenuation were evaluated with a commercially available phantom SO-2 (STC Expert, Moscow, Russia) where the actual parameters are known, which was also routinely used to calibrate the flow detectors. After observing reproducible results in the phantom, we conducted measurements on the samples. The parameters for each material were determined by averaging five measurements.

Experimental procedure

After estimating acoustic parameters, the samples and anatomical phantoms were examined with linear probes on the following ultrasound scanners: Sonoace 8000 EX Prime operating in B-mode; Ruscan 65 M (RPA "Scanner", Moscow, Russia) with LA3-14AD linear probe operating at central frequency of 9.4 MHz (B-mode) and 8 MHz (sonoelastography mode); Angiodin Sono/P-Ultra (BIOS, Moscow, Russia) with L5-12/40 linear probe operating at central frequency of 7.5 MHz (sonoelastography mode); and BK Spectro Ultrasound (BK medical, Herlev, Denmark) with 14L3e linear probe operating at central frequency of 9 MHz (B-Mode). All images were analyzed at depths ranging from 30 to 70 mm. Using each of the scanners, an ultrasonographer with 7 years' of experience captured and stored three images for each sample and lesion in such a way that their borders were visible. For each of the lesions, the ultrasonographer visually assessed the echogenicity and clarity of the borders. The ultrasonographer additionally examined each of the lesions with the Angiodin Sono/P-Ultra scanner in the elastography mode and assessed the strain ratio, which represents under certain assumptions an indirect assessment of tissue stiffness. To visualize the results obtained with the elastographic version of the phantom, a bar plot of stiffness in the form of "average \pm standard deviation" was created based on 9 measurements for each of the Shore scale values.

The relative level of echogenicity for the samples was assessed visually according to the consensus of three ultrasonographers with experience ranging from 7 to 19 years.

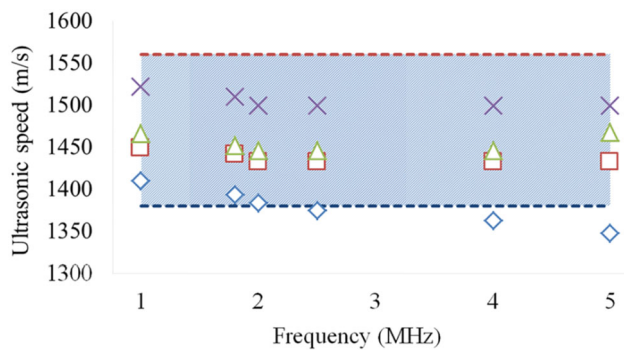


Fig. 5 Frequency dependence of ultrasound speed in the mammary gland (values obtained from [21]): (—) min, (—) max; (◇) pure plastisol from our experiments, (□) a mixture of plastisol and 0.5% graphite powder, (△) a mixture of plastisol and 1% graphite powder, (×) a mixture of plastisol, 1% graphite powder and 0.5% metallic glitter

They ranked the sonograms of the samples in order of increasing echogenicity; thus, they formed a grayscale palette for ranking the echogenicity of lesions.

To assess the models of lesions, clinical feedback was obtained in terms of a survey. The participants were students studying ultrasonography (19 participants), and ultrasonographers with different level of experience: from 0 to 3 years (4 participants), from 4 to 10 years (2 participants), from 10 to 20 years (2 participants), and more than 20 years (1 participant). They were asked to find each of the modeled inclusions in the differential version of the phantom and grade how close the models of inclusions replicate real inclusions on a scale from 0 to 10, where 10 being “very close”. The results were presented in form of a bar plot.

Results

Figure 1 shows the result of choosing admixtures to reproduce different levels of echogenicity. It can be noted that we managed to model 4 levels. Therefore, we evaluated echogenicity on a scale from 1 to 4, with 1 being anechoic and 4 being hyperechoic.

Figure 5 shows the dependency of sound speed on frequency for plastisols with various admixtures. We borrowed the minimum and maximum levels of the sound speed in human mammary gland from the literature [21]. Figure 5 reflects the range of speed of sound found in the fatty and glandular tissues. We also evaluated the attenuation at the frequency of 1 MHz, which was 0.05 dB/cm/MHz in plastisol with the Shore stiffness of 11 units without admixture, the attenuation increased to 0.18 dB/cm/MHz with the addition of 0.5% graphite powder, up to 0.22 dB/cm/MHz with the addition of 1% graphite powder, and up to 0.45 dB/cm/MHz with the addition of 1% graphite powder and 0.5% metallic glitter.

Based on the echograms of the basic, differential and elastographic versions of the phantom presented in Figs. 6, 7, 8 and 9, we can observe that the background tissue is homogeneous and the lesions’ borders are quite clear; the clarity is, especially pronounced in Fig. 9b, obtained at the higher carrier frequency.

Figure 7 shows typical images of the main lesions in the differential version of the phantom. The strain ratios for the presented masses, namely hyperechoic (a replication of lipoma), hypoechoic (a replication of malignant tumor), and hypoechoic (a replication of fibroadenoma) were 0.39, 4.26, and 0.83, respectively. The presented in Fig. 7a, a replica of lipoma consists of plastisol with a Shore stiffness of 6 units with the addition of 1% graphite powder and 0.5% metallic glitter. The replica of malignant tumor (Fig. 7b) is from plastisol with the Shore stiffness of 17 units without admixture. The replica of fibroadenoma (Fig. 7c) is from plastisol with the Shore stiffness of 11 units with addition of 0.5% graphite powder. To assess the realism of the inclusion models, a survey among ultrasound professionals and students was conducted. Its results in the form of “average \pm standard deviation” are presented in Fig. 8.

Figures 9 and 10 show examples of sono- and elastograms of typical lesions in the elastographic version of the phantom. Lesion made of the softest plastisol with a Shore stiffness of 3 units with the addition of 1% graphite powder, is shown in Fig. 10a, that had a strain ratio of 0.65. The hardest lesion shown in Fig. 10b, plastisol with a Shore stiffness of 17 units and without admixture had a strain ratio of 4.98. Such stiffness indicators demonstrate that the lesion shown in Fig. 10a is softer, and the other lesion shown in Fig. 10b, respectively, is harder than the surrounding tissue, which is made of plastisol with the Shore stiffness of 6 units with 1% graphite powder and 0.5% metallic glitter.

Figure 11 represents the data obtained with 3 experienced ultrasonographers measuring elasticity in elastographic version of the phantom. Targets with known equal stiffness presented in Shore scale values were grouped. For each of the group there is a bar in Fig. 11.

Discussion

The developed phantom is a simplified model of the human mammary gland. We simulated the breast’s glandular tissue and lesions with a mixture of polyvinyl chloride plastisol, graphite powder, and glitter at various concentrations. Figure 5 shows that the longitudinal ultrasonic speed is 1408 m/sec at the frequency of 1 MHz for pure plastisol with a Shore stiffness of 11 units. The addition of 0.5% graphite powder increases the speed up to 1449 m/sec, which is close to the reported value measured in the fresh sample of breast fat [22]. The addition of 1% graphite powder increases it

Fig. 6 Ultrasound images of masses in the basic version of the phantom, obtained with Sonoace 8000 EX Prime: **a** anechoic mass in the form of a letter “E”; **b** hyperechoic mass in the form of a star; **c** hyperechoic mass in the form of a plus; **d** hyperechoic mass in the form of a fish

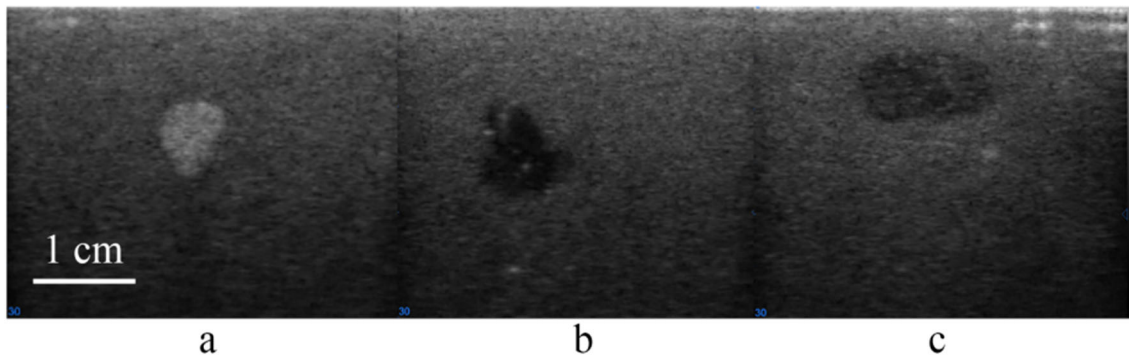
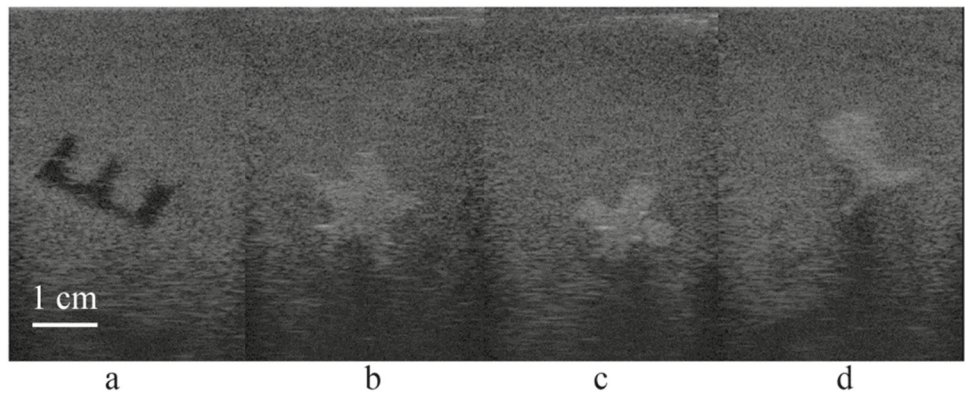


Fig. 7 Ultrasound images of lesions of the differential version of the phantom obtained with Sonoace 8000 EX Prime: **a** hyperechoic lesion with clear, smooth margins and a weak distal acoustic shadow is a replica of lipoma; **b** hypoechoic lesion of the vertical spatial orientation with

fuzzy irregular margins is a replica of malignant tumor; **c** hypoechoic lesion of the horizontal spatial orientation with clear, smooth margins and slight distal acoustic enhancement is a replica of fibroadenoma

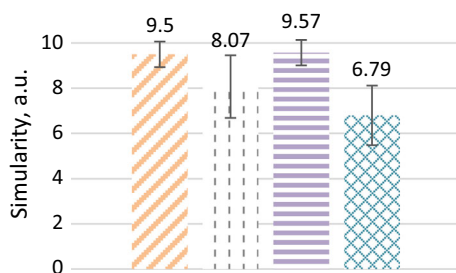


Fig. 8 Distribution of survey answers regarding the similarity of the models with their prototypes encountered on sonograms in clinical practice: (left to right) cyst, fibroadenoma, lipoma, and malignant tumor

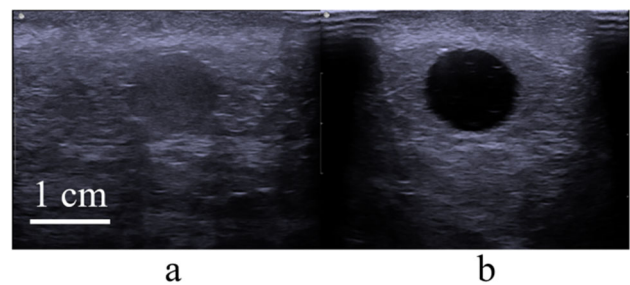


Fig. 9 Ultrasound images of lesions in the elastographic version of the phantom, obtained with BK Specto Ultrasound scanner: **a** lesion with level 3 echogenicity; **b** lesion with level 1 echogenicity

further to 1465 m/sec. The addition of 0.5% metallic glitter creates the highest echogenicity and gives the ultrasonic speed of 1522 m/sec. All these values correspond to the published results for a mixture of plastisol [11] and fall within the normal range for breast tissues [21], which allows trainees to have correct feedback regarding the targeting of the lesions for biopsy. The ultrasonic speed in the basic and differential versions of the phantom is approximately 1% less than the longitudinal ultrasonic speed in the biological adipose tissue, and the ultrasonic speed in the elastographic version is 1.4%

less than the ultrasonic speed in the glandular tissue [8, 15]. The differences in the longitudinal ultrasonic speed between adipose and glandular tissues reported in the literature [23] are 3.8–8.1% and can cause aberrations in the ultrasound examination, leading to a deterioration in resolution [24]. In the developed phantom, these effects of image degradation were not registered.

This is the first study that presents a polyvinyl chloride plastisol-based breast phantom that used metallic glitter as a

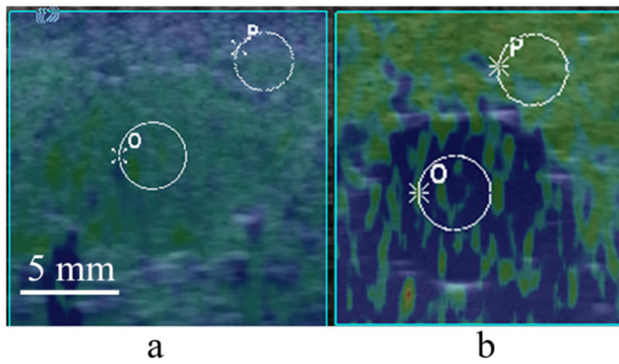


Fig. 10 Compression elastograms of lesions in the elastographic version of the phantom obtained with the Angiodin Sono/P-Ultra ultrasound scanner: **a** a soft mass; **b** a hard mass

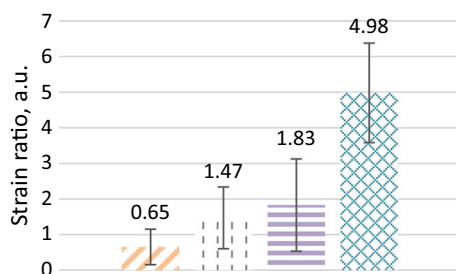


Fig. 11 Strain ratio measured in elastographic version of the phantom with ultrasound scanner in elastography mode for targets made of material which hardness is characterized by either of 4 Shore values: (left to right) 3, 9, 11 and 17 units on the Shore scale

scatterer. The results show that this scatterer is very promising, because the speckle pattern of the ultrasonic images obtained is very close to the pattern obtained in the human breast.

Since the basic version of the phantom contains a set of masses with easily recognizable shapes (Figs. 2b, 6), it is convenient for developing the manual skills in finding the right probe position to visualize a mass in the desired slice. In clinical practice, an ultrasonographer observes a lesion for several months by asking the patient to visit regularly. During each subsequent visit, the ultrasonographer tries to position a transducer at exactly the same location as before to correctly compare the dimensions of the suspicious lesion and assess its growth.

While previously reported lesion models [11] mimic real lesions by reproducing their echogenicity level, manufacturing the differential phantom, we tried to reproduce other known ultrasound signs of focal lesions [25] as well. For example, a typical breast lipoma is characterized by increased echogenicity compared to the surrounding adipose tissue at the superficial location and low stiffness during elastography. In the case of a prolonged existence of lipoma and calcification of the capsule behind the lesion, an artifact of

acoustic shadow may occur. As can be seen in Fig. 7a, the model of lipoma has the described features of the real foci. A typical fibroadenoma is characterized by the oval or round shape, horizontal spatial orientation, clear margins, lobular structure, often with a thin rim and posterior acoustic amplification, as shown in Fig. 7c. In case of suspicion for breast cystic lesion (Fig. 9b), the following signs are seen in the sonogram: a rounded anechoic structure with clear, smooth margins. Thus, the differential version of the breast phantom allows developing skills of assessing and reporting parameters of various masses that mimic the encountered in clinical practice focal breast lesions. As can be seen from the result of the survey conducted among ultrasonography students and experienced professionals, presented in Fig. 8, the models of inclusions in this phantom are relatively accurate with the models of cyst and lipoma being the most realistic.

The elastographic version will help students to get a better grasp of the ultrasound elastography (Fig. 10), since this version contains lesions that look similar in the B-mode, but differ from each other and the surrounding tissues in terms of stiffness. As can be seen in Fig. 11, the increase in the Shore stiffness values leads to higher stiffness measured with the ultrasound scanner. The elastographic version also differs from other versions in modeling a background by softer plastisol and a mixture of metallic glitters, which makes it the most echogenic, corresponding to level 4 on the echogenicity scale (Fig. 1d). According to the ultrasonographers participating in the study, this background is the closest to the real ultrasound image of the breast.

For training using the phantom, we propose the following steps:

- (1) Select one of the lesion models in the diagram shown in Fig. 2.
- (2) Pick up the phantom, apply the gel, position a linear probe on the surface of the phantom so that a sonogram of the phantom can be observed on the scanner's screen.
- (3) By looking at the scanner's screen, observe the lesion models presented in the phantom and find the one you selected.
- (4) Using a measuring tool available in the scanner's interface, estimate the dimensions of the selected model.
- (5) Insert the ultrasound-guided needle so that it passes through the wall inside the selected model.
- (6) Based on the assessment results of the model size, as well as the speed and number of attempts required for a needle penetration of the wall of the selected model, evaluate the skill of ultrasound-guided manipulation.

Our experience of working with plastisol has indicated that it interacts chemically with some plastics, which was also noted in the literature [11]. Previously, we tried to make molds from ABS plastic, which proved well when working

with agar and gelatin, however, it turned out that plastisol dissolves ABS plastic but not PLA. That is why we have decided to print molds using PLA plastic. Unlike agar and gelatin, plastisol retains its properties over the years; moreover, it is a wear-resistant and easy to use material, which makes plastisol attractive for manufacturing training phantoms.

A limitation of our phantom design includes the fact that the modeled cysts do not contain liquid. They can be punctured with a needle, but the liquid cannot be pumped out. A positive side of this design is that cyst models, like other lesions, can be punctured multiple times. Another limitation compared to the phantom developed by De Matheo et al. [13] is the absence of lactiferous ducts. Thus, in the future, we plan to complicate the breast phantom by including models of adipose and glandular tissues, as well as lactiferous ducts and ductal carcinoma.

Conclusion

The methodology described in this article allows creating a breast phantom and can be easily replicated in any laboratory. Using this methodology, three breast phantoms were designed to train and improve the skills of performing ultrasound examinations, namely the basic, differential and elastographic phantom. The basic one contains 12 masses with easily recognizable shapes. It allows the development of hand–eye coordination, which is so critical for an ultrasound specialist. In addition, it is the ideal tool for teaching to find the correct probe position to visualize the mass in the desired slice. The differential one contains masses that mimic breast lesions in various shapes, stiffnesses and echogenicities: lipoma, fibroadenoma, cyst, malignant tumor. This phantom was designed to practice the skills of interpretation and differential ultrasound diagnosis of breast lesions. The elastographic one contains spherical masses of various stiffness and is intended for practicing the usage of elastography. These phantoms are needle permeable and can be used not only for elastography and hand–eye coordination training, but also for practicing ultrasound-guided biopsy skills.

Acknowledgment This paper was prepared by a group of authors as a part of the research and development effort titled “Development of design and manufacturing technology, and production of phantoms to capture more mineable data from ultrasound imaging”, (USIS No. 123031500001-4) in accordance with the Order No. 1196 dated December 21, 2022 “On approval of state assignments funded by means of allocations from the budget of the city of Moscow to the state budgetary (autonomous) institutions subordinate to the Moscow Health Care Department, for 2023 and the planned period of 2024 and 2025” issued by the Moscow Health Care Department.

Declarations

Conflict of interest The authors declare that they have no conflict of interest or personal relationships that could have appeared to influence the work reported in this paper.

References

- Berg WA, Gutierrez L, NessAiver MS, Carter WB, Bhargavan M, Lewis RS, Ioffe OB (2004) Diagnostic accuracy of mammography, clinical examination, US, and MR imaging in preoperative assessment of breast cancer. *Radiology* 233(3):830–849. <https://doi.org/10.1148/radiol.2333031484>
- Carton AK, Bakic P, Ullberg C, Derand H, Maidment AD (2011) Development of a physical 3D anthropomorphic breast phantom. *Med Phys* 38(2):891–896. <https://doi.org/10.1118/1.3533896>
- Schmidt G, Gerlinger C, Endrikat J, Gabriel L, Müller C, Baus S, Volk T, Sebastian Findekleef EF, Solomayer A, Hamza RS (2021) Teaching breast ultrasound skills including core-needle biopsies on a phantom enhances undergraduate student’s knowledge and learning satisfaction. *Arch Gynecol Obstet* 304:197–202. <https://doi.org/10.1007/s00404-021-06016-8>
- Browne JE, Gu C, Fazzi RT, Fagan AJ, Tradup DJ, Hangian-dreou NJ (2019) Use of novel anthropomorphic breast ultrasound phantoms for radiology resident education. *J Am Coll Radiol* 16(2):211–218. <https://doi.org/10.1016/j.jacr.2018.08.028>
- Schwartz CM, Ivancic RJ, McDermott SM, Bahner DP (2020) Designing a low-cost thyroid ultrasound phantom for medical student education. *Ultrasound Med Biol* 46(6):1545–1550. <https://doi.org/10.1016/j.ultrasmedbio.2020.01.033>
- Leonov DV, Kulberg NS, Gromov AI, Morozov SP (2020) Detection of microcalcifications using the ultrasound Doppler twinkling artifact. *Biomed Eng* 54:174–178. <https://doi.org/10.1007/s10527-020-09998-y>
- Leonov DV, Kulberg NS, Gromov AI, Morozov SP, Vladzimirskiy AV (2018) Diagnostic mode detecting solid mineral inclusions in medical ultrasound imaging. *Acoust Phys* 64:624–636. <https://doi.org/10.1134/S1063771018050068>
- Ruvio G, Solimene R, Cuccaro A, Fiaschetti G, Fagan AJ, Cour-nane S, Cooke J, Ammann MJ, Tobon J, Brown JE (2020) Multimodal breast phantoms for microwave, ultrasound, mammography. *Magn Reson Comput Tomogr Imaging Sens* 20(8):2400. <https://doi.org/10.3390/s20082400>
- Usumura M, Kishimoto R, Ishii K, Hotta E, Kershaw J, Higashi T, Obata T, Suga M (2021) Longitudinal stability of a multi-modal visco-elastic polyacrylamide gel phantom for magnetic resonance and ultrasound shear-wave elastography. *PLoS ONE* 16(5):e0250667. <https://doi.org/10.1371/journal.pone.0250667>
- He Y, Liu Y, Dyer BA, Boone JM, Liu S, Chen T, Zheng F, Zhu Y, Sun Y, Rong Y, Qiu J (2019) 3D-printed breast phantom for multi-purpose and multi-modality imaging. *Quant Imaging Med Surg* 9(1):63–74. <https://doi.org/10.21037/qims.2019.01.05>
- Carvalho IM, Matheo LL, Silva JF, Costa JF, Borba CM, Krüger MA, Infantsi AF, Pereira WC (2016) Polyvinyl chloride plastisol breast phantoms for ultrasound imaging. *Ultrasonics* 70:98–106. <https://doi.org/10.1016/j.ultras.2016.04.018>
- Madsen EL, Zagzebski JA, Frank GR (1982) An anthropomorphic ultrasound breast phantom containing intermediate-sized scatterers. *Ultrasound Med Biol* 8:381–392

13. Matheo LL, Geremia J, Calas MJ, Costa JF, Silva FF, Krüger MA, Pereira WC (2018) PVC-based anthropomorphic breast phantoms containing structures similar to lactiferous ducts for ultrasound imaging: a comparison with human breasts. *Ultrasonics* 90:144–152. <https://doi.org/10.1016/j.ultras.2018.06.013>
14. Madsen EL, Zagzebski JA, Frank GR, Greenleaf JF, Carson PL (1982) Anthropomorphic breast phantoms for assessing ultrasonic imaging system performance and for training ultrasonographers: part II. *J Clin Ultrasound* 10:91–100
15. Chatelin S, Breton E, Arulrajah A, Giraudeau C, Wach B, Meylheuc L, Vappou J (2020) Investigation of PolyVinyl chloride plastisol tissue-mimicking phantoms for MR- and ultrasound-elastography. *Front Phys* 8:577358. <https://doi.org/10.3389/fphy.2020.577358>
16. Ustbas B, Kilic D, Bozkurta A, Aribal ME, Akbulut O (2018) Silicone-based composite materials simulate breast tissue to be used as ultrasonography training phantoms. *Ultrasonics* 88:9–15. <https://doi.org/10.1016/j.ultras.2018.03.001>
17. Vogt WC, Jia C, Wear KA, Garra BS, Joshua PT (2016) Biologically relevant photoacoustic imaging phantoms with tunable optical and acoustic properties. *J Biomed Opt* 21(10):101405. <https://doi.org/10.1117/1.JBO.21.10.101405>
18. STL files for 3D printing breast phantom molds. https://www.researchgate.net/publication/362606799_STL_files_for_3D_printing_breast_phantom_molds
19. Schey JA (2000) Introduction to manufacturing processes, 3rd edn. The McGraw-Hill Companies
20. Leonov D, Kodenko M, Leichenko D, Nasibullina A, Kulberg N (2022) Design and validation of a phantom for transcranial ultrasonography. *Int J Comput Assist Radiol Surg*. <https://doi.org/10.1007/s11548-022-02614-2>
21. Bamber JC (1983) Ultrasonic propagation properties of the breast. In: Jellins J, Kobayachi T (eds) Ultrasonic examination of the breast. J. Wiley and Sons, New York, pp 37–44
22. Keijzer L, Lagendijk M, Stigter N, van Deurzen CHM, Verhoef C, van Lankeren W, Koppert LB, van Dongen KWA (2018) Measurement of the speed of sound, attenuation and mass density of fresh breast tissue. In: Proceedings of the international workshop on medical ultrasound tomography, pp 369–384
23. Rumack CM, Wilson SR, Charboneau JW, Levine D (2011) Diagnostic ultrasound, 4th edn. Mosby Elsevier, Philadelphia
24. Osipov LV, Kulberg NS, Skosyrev SV, Leonov DV, Grigoriev GK, Vladzimirskiy AV, Morozov SP (2021) Transcranial beam steering with aberration correction. *Biomed Eng* 54(6):438–442. <https://doi.org/10.1007/s10527-021-10057-3>
25. Bevers TB, Helvie M, Bonaccio E, Calhoun KE, Daly MB, Farrar WB, Garber JE, Gray R, Greenberg CC, Greenup R, Hansen NM, Harris RE, Heerdt AS, Helsten T, Hodgkiss L, Hoyt TL, Huff JG, Jacobs L, Lehman CD, Monsees B, Niell BL, Parker CC, Pearlman M, Philpotts L, Shepardson LB, Smith ML, Stein M, Tummyan L, Williams C, Bergman MA, Kumar R (2018) Breast cancer screening and diagnosis. NCCN Clinical practice guidelines in oncology. *J Natl Compr Canc Netw* 16(11):1362–1389. <https://doi.org/10.6004/jnccn.2018.0083>

Publisher's Note Springer Nature remains neutral with regard to jurisdictional claims in published maps and institutional affiliations.

Springer Nature or its licensor (e.g. a society or other partner) holds exclusive rights to this article under a publishing agreement with the author(s) or other rightsholder(s); author self-archiving of the accepted manuscript version of this article is solely governed by the terms of such publishing agreement and applicable law.

Author and Affiliations

Denis Leonov^{1,2}  · Daria Venidiktova³  · José Francisco Silva Costa-Júnior⁴  · Anastasia Nasibullina^{1,2}  · Olga Tarasova⁵ · Kristina Pashinceva⁶ · Natalia Vetsheva⁷  · Julia Bulgakova^{1,2}  · Nicholas Kulberg⁸  · Alexey Borsukov³  · Manob Jyoti Saikia⁹ 

✉ Denis Leonov
strat89@mail.ru

Daria Venidiktova
daria@venidiktova.ru

José Francisco Silva Costa-Júnior
francisco@sbeb.org.br

Anastasia Nasibullina
NasibullinaAA@zdrav.mos.ru

Natalia Vetsheva
n.vetsheva@mail.ru

Julia Bulgakova
BulgakovaYV@zdrav.mos.ru

Alexey Borsukov
bor55@yandex.ru

¹ Moscow Center for Diagnostics and Telemedicine, Moscow, Russia

² Moscow Power Engineering Institute, Moscow, Russia

³ Smolensk State Medical University, Moscow, Russia

⁴ Brazilian Air Force Academy, Pirassununga, São Paulo, Brazil

⁵ Plekhanov Russian University of Economics, Moscow, Russia

⁶ Moscow State University of Medicine and Dentistry, Moscow, Russia

⁷ Federal State Budgetary Educational Institution of Further Professional Education “Russian Medical Academy of Continuous Professional Education” of the Ministry of Healthcare of the Russian Federatio, Moscow, Russia

⁸ Federal Research Center “Computer Science and Control” of the Russian Academy of Sciences, Moscow, Russia

⁹ Department of Electrical Engineering, University of North Florida, Jacksonville, FL 32224, USA